

Contribution by different marine bacterial communities to particulate beam attenuation

Martin A. Montes-Hugo^{1,*}, Hugh Ducklow², Oscar M. Schofield¹

¹Coastal Ocean Observation, Institute of Marine and Coastal Sciences, Rutgers University, New Jersey 08901-8521, USA

²The Ecosystems Center, Marine Biological Laboratory, Woods Hole, Massachusetts 02543, USA

ABSTRACT: Contribution of heterotrophic marine bacteria (HB) to the particulate beam attenuation coefficient (c_p) was estimated as a function of latitude in diverse marine regions. Calculations were based on surface measurements (0 to 20 m depth) of bacterial abundance and biovolume, physio-optical empirical relationships, and light scattering models. Relative contribution of spherical HB to c_p (c_{HB}/c_p) was commonly below 10%, and slightly increased (~3%) when bacterial shape was assumed to be cylindrical. HB accounted for a larger fraction of c_p magnitude at lower latitudes because of the greater abundance of bacteria. HB explained about a third of c_p spatial variability in Antarctic (Antarctic Polar Front, Ross Sea) and non-polar (equatorial Pacific Ocean, Arabian Sea) oceanic regions.

KEY WORDS: Heterotrophic marine bacteria · Particulate beam attenuation coefficient · Light scattering · Mie theory · Polar environments

Resale or republication not permitted without written consent of the publisher

INTRODUCTION

Beam transmissometers are a common instrument on oceanographic cruises as several important biochemical parameters, e.g. particulate organic carbon (POC) (Bishop 1999, Behrenfeld & Boss 2006), and biological parameters, e.g. chlorophyll *a* (chl) concentration (Loisel & Morel 1998), are estimated from the particulate beam attenuation coefficient (c_p). Since heterotrophic marine bacteria (HB) and phytoplankton dominate light scattering in the open ocean (Stramski & Kiefer 1991), and c_p is mainly determined by particulate scattering (Bricaud et al. 1988), relationships between c_p and HB could be anticipated. Detritus (non-living organic and mineral particles) is probably another important optical constituent contributing to c_p magnitude (30 to >50%) (DuRand & Olson 1996, Claustre et al. 1999, Stramski et al. 2001, Green et al. 2003, Oubelkheir et al. 2005, Grob et al. 2007). However, calculation of this contribution is very uncertain and results in very small (~0) or large (>total c_p) estimates. Based on empirical functions between HB abundance (BA) and chl (Cole et al. 1988), Morel & Ahn (1990) proposed a power type relationship be-

tween scattering coefficient of HB ($b_{HB} = c_{HB} - a_{HB}$, where a_{HB} = particulate absorption coefficient of HB ≈ 0 , Table 1) and chl. A correlation between HB abundance and c_p as a function of depth was evident in Peruvian coastal waters (Tau correlation coefficient = 0.295 to 0.646) (Spinrad et al. 1989a). Despite this established linkage between c_p and HB, these relationships may not be universal as several studies report a lack of dependency between BA and chl (Bird & Karl 1999, Duarte et al. 2005). Given this, the question therefore arises: To what extent can HB concentration be estimated from c_p measurements?

In general, influence of HB on c_p magnitude is variable (0.05 to 0.5% of c_p) (Chung et al. 1996, DuRand & Olson 1996, Green et al. 2003, Oubelkheir et al. 2005) and is inversely related to phytoplankton biomass (e.g. oligotrophic waters: up to 50%; eutrophic waters: up to 5%) (Stramski & Kiefer 1991, Grob et al. 2007). Based on bacterial incubations (lab cultures and mesocosms) or field samples collected in different oceanic environments, the proportion of c_p contributed per bacterial cell varies by a factor of 20 (1×10^{-14} to $1.8 \times 10^{-13} \text{ m}^{-1} \text{ cell}^{-1}$). This large variance in the scattering cross sec-

*Email: montes@marine.rutgers.edu

tion per spherical bacterium (σ_{HB} , Table 1) reported in the literature is partially related to methodological differences in calculating c_{HB} . Approaches to compute c_{HB} differ regarding assumptions (e.g. constant versus variable parameterization) about HB cell size (Chung et al. 1998, Green et al. 2003, Oubelkheir et al. 2005) and the real part of the refractive index (n_{HB}) (Chung et al. 1998, Green et al. 2003), trophic status of HB during incubation experiments (Stramski & Kiefer 1998) and theories (e.g. exact versus approximate) used to derive σ_{HB} and scattering efficiencies of HB (Q_{HB}) (DuRand & Olson 1996, Chung et al. 1998, Green et al. 2003, Grob et al. 2007). The wide range of σ_{HB} values between studies may also respond to natural variability between oceanic areas with distinct hydrographic and nutrient regimes. These environmental conditions are expected to affect σ_{HB} by altering bacterial cell size, shape and chemical composition (Stramski & Kiefer 1991, 1998).

The aforementioned uncertainties on how HB affect c_{p} variability and magnitude in marine waters can be better constrained by standardizing the calculation of c_{HB} and having a more representative characterization of bacterial assemblages inhabiting the oceanic domains. With this in mind, the objective of the present study was to answer the following questions: (1) Is c_{p} more sensitive to optical contribution of HB in Antarctic or non-polar waters? (2) To what extent is there spatial covariation of c_{p} , HB and chl when comparing Antarctic and non-polar surveys? (3) Which attribute of bacteria (BA, n_{HB} , cell size or shape) dominates c_{p} response as a function of latitude? We hypothesized

that contribution of HB to c_{p} magnitude and horizontal variability is larger in non-polar surveys with respect to those conducted in Antarctic waters due to the greater abundance of HB at low and mid latitudes.

MATERIALS AND METHODS

Surface measurements (average within 0 to 20 m depth) of c_{p} ($\lambda = 660 \text{ nm}$), number of bacterial cells per unit of volume (BA), biovolume per cell (BV) and chl were obtained from 10 oceanographic cruises conducted during the Joint Global Ocean Flux Study (JGOFS, www.whoi.edu/) project. The surveys were representative of low (5°N to 5°S , equatorial Pacific Ocean, EQP), mid (10°N to 22.5°N , Arabian Sea, ARAB), and high (50.2°S to 70.4°S , Antarctic Polar Front, APF; 73.5°N to 78.0°S , Ross Sea, RS) latitude environments. Overall, the datasets encompassed waters with different trophic states (chl range 0.01 to 13.02 mg m^{-3}) and ocean conditions (monsoon versus intermonsoon regime, El Niño warm versus cold phase), and sites were predominantly oceanic except in RS surveys where some locations were influenced by coastal shelf features. For each sampling station, the average of each variable was calculated along the vertical, and comparisons between c_{p} , chl, and HB parameters were performed with data collected less than 4 h apart. For all cruises, the average coefficient of variation (%CV = $100 \times \text{SD}/\text{mean}$) of c_{p} , chl, BV and BA measurements between 0 and 20 m depth was 7.1, 16, 9.5, and 12.5%, respectively.

In all cases, c_{p} was derived from light transmission values (RS, EQP, ARAB: path length = 0.25 m; APF: path length = 0.20 m; accuracy $\sim 0.005 \text{ m}^{-1}$, sensitivity = 0.0012 m^{-1}) (Spinrad et al. 1989b, Bishop 1999). Raw transmission data from SeaBird CTD files were averaged at 1 to 2 dB intervals and spikes were removed. Sea Tech transmissometers were calibrated by the manufacturer to have a total beam attenuation in particle-free seawater (c_w) of 0.364 m^{-1} . A different transmissometer was used (WetLabs) only during APF-2, but its measurements were matched with Sea Tech using an offset of 0.0151 m^{-1} following JGOFS protocols (<http://usjgofs.whoi.edu/jg/dir/jgofs>). Values of total beam attenuation (c) were detrended from the decay of the transmissometer light-emitting diode (LED) during each survey. The data were also adjusted for factory and cruise air calibrations and

Table 1. Definitions of abbreviations, symbols and terms used throughout the text

Symbol	Definition	Units
HB	Heterotrophic marine bacteria	
pdf	Probability distribution function	Dimensionless
ADT	Anomalous diffraction theory	
GRA	Gaussian-Ray approximation	
d	Mean cell diameter of bacteria	μm
BA	Bacteria abundance per unit of volume	cells m^{-3}
BV	Average biovolume per cell	μm^3
λ	Light wavelength	μm
α	Size parameter	Dimensionless
ρ	Phase shift	Dimensionless
c_{p}	Particulate beam attenuation coefficient	m^{-1}
c_{HB}	Particulate beam attenuation due to spherical HB	m^{-1}
σ_{HB}	Scattering cross section per spherical bacterium	$\text{m}^2 \text{ cell}^{-1}$
$\sigma_{\text{HB}}^{\text{cyl}}$	Scattering cross section per cylindrical bacterium	$\text{m}^2 \text{ cell}^{-1}$
Q_{HB}	Scattering efficiency factor	Dimensionless
Q_c	Attenuation efficiency factor for heterotrophic bacteria	Dimensionless
S_{HB}	Geometrical cross section of spherical HB	m^2
$S_{\text{HB}}^{\text{cyl}}$	Geometrical cross section of cylindrical HB	m^2
n_{HB}	Real part of refractive index of HB relative to seawater	Dimensionless
n_w	Real part of refractive index of seawater	Dimensionless
PCSA	Particle cross-sectional area per m^3	m^{-1}

corrected for changing temperature, salinity, pressure and refractive index of seawater. For each cast, c_p was calculated by subtracting c_w and adding an offset value related to the minimum value of c_p measured between 0 and 400 m stations (Chung et al. 1996). This offset is obtained from the intercept of c_p as a function of POC stations (JGOFS protocols), and provides consistency between c_p profiles since systematic biases are eliminated (e.g. signal drift, incomplete cleaning of optical windows, change of sensor). For all datasets, bias to c_p due to incomplete correction by light absorption of yellow substances is expected to be minimal at a wavelength of 660 nm since the absorption coefficient of chromophoric dissolved compounds (a_g) at that wavelength always represented a small fraction of c_p (0.05 to 1.5%; SeaBass, NASA, <http://seabass.gsfc.nasa.gov>). In Antarctic waters, a_g/c_p at 660 nm are commonly less than 0.3% and corresponded to the lower range of c_{HB}/c_p calculated for RS and APF.

BA and BV values were estimated using digital image analysis of video microscopic images of bacterial, cellular perimeter and area (JGOFS cruises) (Baldwin & Bankston 1988, Knap et al. 1994). Typical precision of BA and BV measurements using video images is 5% (Bjørnsen 1986). Based on microscopic sizing of fluorescent latex beads, accuracy of BV is expected to be close to 10% (Bjørnsen 1986). In general, most of the HB estimations represent the bulk community of HB as a whole; thus, they do not make a distinction between free-living and particle-attached assemblages. However, most of HB are expected to be free-living bacteria, as underestimation of BA due to particle-attached bacteria is commonly less than 10% (H. Ducklow pers. obs.). For all cruises, chl concentrations were measured *in situ* using a fluorometer previously calibrated (sensitivity $\sim 0.01 \mu\text{g l}^{-1}$) with discrete samples (JGOFS protocols, W. Gardner pers. comm.).

Models to estimate partial contribution of HB to c_p .

Non-pigmented bacteria have only a minimal absorption of photons in the spectral range of 406 to 415 nm, which is probably due to the Soret band of respiratory cytochromes (Stramski & Kiefer 1998). Therefore, at a wavelength of 660 nm, a_{HB} approximates 0 ($\sim 10^{-4} \text{ m}^{-1}$) and c_{HB} is approximately equal to b_{HB} (Morel & Ahn 1990) (Table 1) as follows:

$$c_{HB} = b_{HB} = BA \times S_{HB} \times Q_{HB} \quad (1)$$

where BA is bacterial abundance per unit of volume, S_{HB} is the geometric cross section ($\pi/4 \times d^2$, where d is diameter of the cell in m, $d = 2 \times [(3/4) BV/\pi]^{1/3}$), Q_{HB} is the dimensionless scattering efficiency factor (Van de Hulst 1957), and $S_{HB} \times Q_{HB}$ is the scattering cross section (σ_{HB}). Note that BA, S_{HB} , Q_{HB} , and σ_{HB} represent averaged values for each location and are calculated for a community of spherical HB composed of organ-

isms with different refractive indices m ($m = n - i \times n'$, where $i^2 = -1$ and n and n' are the real and imaginary parts, respectively). The term m is relative with respect to the refractive index of pure seawater (n_w), and for HB, $m \cong n \cong 1$ and n' is close to 0. Based on this simplification, the anomalous diffraction theory (ADT, Van de Hulst 1957) can be applied to estimate Q_{HB} of homogeneous and non-absorbing microspheres as follows:

$$Q_{HB}(\rho) = Q_c(\rho) = 2 - (4/\rho) \sin \rho + (4/\rho^2) (1 - \cos \rho) \quad (2)$$

$$\rho = 2 \alpha (n_{HB} - 1) \quad (3)$$

and

$$\alpha = (\pi d/\lambda_0) n_w \quad (4)$$

where α is a dimensionless size parameter, λ_0 is the wavelength *in vacuo* (0.66×10^{-6} m), n_w depends on sea surface temperature and salinity (Quan & Fry 1995) and ρ (phase lag) is another dimensionless parameter. Note that Eqs. (3) & (4) are valid for a single size class of particles or particles with a very narrow range of diameters like HB. For all surveys, the real part of the refractive index of HB (n_{HB}) was derived empirically as a function of HB diameter (μm) (Stramski & Kiefer 1990) according to the relationship:

$$n_{HB} = 1 + 0.025 d^{-1.2} \quad (r^2 = 0.99) \quad (5)$$

This relationship is based on cellular water content (by vol.) between 55 and 75% and cell volume measurements obtained from 3 bacterial cultures (Simon & Azam 1989). In general, smaller bacterial cells (high n_{HB} values) are more dehydrated and have a larger proportion of volume occupied by proteins than bigger bacterial cells (low n_{HB} values). Based on bacterial intracellular carbon content (C_{CELL}), n_{HB} can also be inversely related to water content per cell (V_w , Morel & Ahn 1990).

Given that C_{CELL} is generally more variable (>5-fold) than C/N (~ 1.5 -fold), n_{HB} can be modeled as a linear function of C_{CELL} ($n_{HB} = 1 + 0.233 \times 10^{-3} C_{CELL}$, Morel & Ahn 1990). Likewise, and assuming a constant density of dry organic matter (ρ_0), C_{CELL} is inversely related to V_w [$C_{CELL} = (1 - V_w) \rho_0$] (Morel & Ahn 1990). Since V_w is directly related to BV and d (assuming a spherical shape) ($V_w = 1.0515 d^{0.6104}$, $r^2 = 0.92$, $n = 7$, Simon & Azam 1989), it is deduced that smaller bacterial cells will be, on average, more efficient at scattering light (high n_{HB} , low V_w) due to a higher C_{CELL} . Characteristic relative errors for lab determinations of n_w and n_{HB} are 0.02 (Quan & Fry 1995) and 0.1% (Jonasz et al. 1997), respectively.

In general, calculation of optical parameters of HB derived from the above equations assumes a community of unattached and free-floating HB. Field studies across different oceanic regions support this view (Wiebe & Pomeroy 1972, Sieburth et al. 1974). Eventually, a violation of this assumption may occur during

senescent phytoplankton blooms or events characterized by waters with an abundant concentration of detritus and formation of aggregates (Abell & Bowman 2005). Assuming a minimum breakage of micro-aggregates (~5 to 500 μm) during counting, a larger fraction of aggregate-attached HB may decrease c_{HB}/c_p due to underestimation of particle-attached BA (i.e. free-living HB are easier to count). On the contrary, if breakage of micro-aggregates is major, a greater proportion of bacteria bound to aggregates would be counted, and c_{HB}/c_p would increase due to a greater mean cell size of particle-attached HB compared to free-living HB (Grossart et al. 2003).

Total error in S_{HB} , Q_{HB} , σ_{HB} , n_{HB} and c_{HB} calculations was determined based on error propagation theory. To obtain mean relative bias of each HB optical parameter, random absolute bias was generated for BA and d (Monte Carlo simulations, Matlab 7.5). Uncertainty on BA ($d\text{BA}$) was allowed to change, i.e. $(\text{BA} - 0.05\text{BA}) \leq d\text{BA} \leq (\text{BA} + 0.05\text{BA})$. Bias on d depends on bacterial cell size and was obtained from the absolute difference between specified and measured BV (Bjørnsen 1986). To compute n_{HB} , 2 errors were added: one randomly derived from d and the other inherited from the relationship of n_{HB} as a function of d (~0.2238% of n_{HB}) (Stramski & Kiefer 1990).

Scattering cross sections of homogeneous (non-coated) and non-spherical (cylindrical) HB were calculated based on the Gaussian Ray approximation (GRA) (Katz et al. 2003):

$$\sigma_{\text{HB}}^{\text{cylin}} = 32 \times (n_w \times 2\pi^3 \times |n_{\text{HB}} - 1| \times 2r^3l) / (3\lambda_0^2) \quad (6)$$

For randomly oriented bacteria, r and l are the radius and length of the cylinder, respectively. The length of the cylinder was equivalent to the diameter of HB considering a spherical shape ($l = d$) while the cylinder radius was calculated as $l/2.5$ and assuming a cylinder diameter of $0.8l$ (Ulloa et al. 1992). Likewise, the mean projected area or geometrical cross section of bacterial rods was computed according to Cauchy's theorem: $S_{\text{HB}}^{\text{cylin}} = \pi r (r + l)/2$ (Brown et al. 2005). The GRA is a statistical interpretation of ADT that assumes soft particles (n is close to 1). The influence of the bacterial cell wall on c_{HB} calculations is assumed to be minor since most of the bacteria inhabiting marine waters are gram negative with relatively thin cell walls (~5 to 10 nm) (Agogue et al. 2005); thus, scattering properties will depend more on size, shape and refraction index of cells (Katz et al. 2003).

Statistical analysis. Linear regression (type II model) was used to quantify the influence of HB on c_p variability at high, low and mid latitude surveys. Due to the low degrees of freedom of individual surveys, spatial dependency of c_p on c_{HB} was examined by merging multiple datasets. Multiple regression analysis with

forward elimination of continuous predictors (Statistica software v7.1) was applied *a posteriori* to rank the relative contribution of n_{HB} , BV and BA to horizontal variability of c_{HB} . Since n_{HB} and BV are interdependent, relationships between BV and c_{HB} are also implicitly influenced by the chemical composition of bacteria. Latitudinal differences in optical and HB parameters were examined with Student's t -test ($H_0: \mu_{\text{Antarctic}} = \mu_{\text{non-polar}}$) following analysis of homogeneity of variances with an F -test ($H_0: s^2_{\text{Antarctic}} = s^2_{\text{non-polar}}$). Multivariate models were constructed using measurements without distinction by time of day; thus, c_{HB} estimations represented ecological conditions averaged for day and night. Unlike the high latitude datasets, the non-polar group included surveys performed during periods of strong (monsoon season and El Niño cold phase) and weak (El Niño warm phase) or absent (intermonsoon) upwelling conditions. The physical forces triggering intermonsoons (wind reversal) and El Niño warm phase (Kelvin wave propagation) events are different, but in both cases produce a general nutrient depletion in surface layers. Unlike the Arabian Sea, upwelling continues during the warm phase of El Niño but at depths above the nutricline. These events have distinct levels of primary production (Ducklow et al. 1995, 2001a); thus, they are expected to affect the contribution of HB to c_p differently.

RESULTS

Contribution of HB to c_p magnitude

As previous studies have suggested, HB was not the major optical component determining c_p magnitude for any of the regions studied, with a maximum contribution of 19% in the Ross Sea (Table 2). This is considerably lower than theoretical maximum predictions of up to 50% (Stramski & Kiefer 1991). Overall, most of the c_{HB}/c_p values were below 10% (polar, 85.3% of samples, $n = 109$; non-polar, 77.2% of samples, $n = 54$). Average HB contributions to c_p were $8.2 \pm 0.7\%$ (mean \pm 2 SD) in non-polar waters and only $3.7 \pm 0.7\%$ in Antarctic waters (Student's t -statistic = 1.98, $p < 0.01$). Survey-to-survey comparisons also indicated that bacteria of Antarctic marine environments may have c_{HB}/c_p values comparable to low and mid latitude environments during some periods of the year (e.g. RS-3 versus EQP-1). Further analysis relating particle cross-sectional area per unit of volume (PCSA) with c_p and c_p/PCSA confirmed that contribution of HB to c_p in the Southern Ocean is small compared with other particulate components (Appendix 1, Fig. A1). In fact, phytoplankton cells explained a larger variability of c_p in Antarctic waters [$c_p = 0.1903 (\pm 0.007, 1 \text{ SE}) \times \text{chl} +$

0.1518 (± 0.0184), $r^2 = 0.89$, $n = 102$] compared with low and mid latitude surveys [$c_p = 0.0614$ (± 0.0106) \times chl + 0.0798 (± 0.0106), $r^2 = 0.42$, $n = 48$].

In general, for non-polar surveys, intra-cruise (up to 3-fold) and inter-cruise (up to 2-fold) maximum variability of c_{HB}/c_p was comparable (Table 2). Interestingly, maximum values of average c_{HB}/c_p per survey (15.1 to 19%) coincided with the lowest average values of total particulate beam attenuation (e.g. $c_p < 0.1$ m^{-1} in RS-3 and EQP-1). This pattern suggests that c_{HB} is relatively constant in magnitude, and that variability in its percentage contribution is more related to fluctuations in other optical components. Although the data analyzed seem to indicate that HB comprises a larger proportion of c_p during periods with an oligotrophic regime and characterized by reduced upwelling intensity (intermonsoon season, ARAB-1, El Niño warm phase EQP-1) (Table 2), the existence of this pattern requires further verification since the computation error of c_{HB}/c_p in these waters is approximately 10-fold

greater than the observed differences on c_{HB}/c_p due to distinct upwelling conditions or trophic status. For individual cruises, a greater contribution of HB to c_p magnitude was either determined by changes on HB counts (APF), BV (ARAB, EQP) or n_{HB} (RS) (Tables 2 & 3). In general, the low and mid latitude surveys were characterized by a greater average of n_{HB} (1.073 ± 0.005 , mean \pm SE), BA ($9.68 \pm 0.94 \times 10^{11}$ cells m^{-3}) and smaller bacterial diameter ($d = 0.416 \pm 0.013$ μm) compared to n_{HB} (1.060 ± 0.005), BA ($6.12 \pm 0.94 \times 10^{11}$ cells m^{-3}) and d (0.491 ± 0.014 μm) of Antarctic surveys (Student's t -statistic = 1.97, $p < 0.01$; Table 3; Appendix 2, Fig. A2). In general, and as inferred from BV range, variability of BV in surface waters was more uniform in non-polar (0.021 to 0.054 μm^3) compared to Antarctic (0.024 to 0.160 μm^3) surveys (F -statistic = 2.94, $p < 0.01$; Appendix 2, Fig. A2). The influence of bacterial cell shape did not considerably affect the contribution of bacteria to the magnitude of c_p . In general, a microbial population entirely composed of bacterial rods had

Table 2. Contribution of heterotrophic bacteria to c_p magnitude in surface waters (0 to 20 m) of different marine regions. For each cruise, the average and range (minimum–maximum) of surface values (0 to 20 m depth) are indicated in the first and second row, respectively; c_p values were measured at $\lambda = 660$ nm (m^{-1}). chl: chlorophyll a concentration (mg m^{-3}); n : number of observations; Q_{HB} : dimensionless scattering efficiency factor (10^{-2}); σ_{HB} : scattering cross section of HB (m^2 $cell^{-1}$) $\times 10^{-14}$; c_{HB}/c_p (%): percentage of c_p due to HB. Assuming a spherical shape of bacterial cells, relative biases of S_{HB} , Q_{HB} , σ_{HB} and c_{HB} in percentage were ± 0.9 , ± 35.7 , ± 36.8 and ± 36.1 % (Antarctic surveys) and ± 0.8 , ± 31.3 , ± 39.4 and ± 31.7 % (non-polar surveys), respectively. In the Arabian Sea, June to September and September to March coincided with monsoon (wet months, summer) and inter-monsoon (dry months, winter) seasons, respectively. In the equatorial Pacific, August and September 1992 corresponded with the El Niño cold phase

Cruise no. (Dates)	Q_{HB}	σ_{HB}	c_{HB}/c_p (%)	c_p	chl	n
Ross Sea						
RS-1	7.11	1.04	2.1	0.067	0.13	18
Oct–Nov 1996	(6.57–7.41)	(0.90–1.20)	(0.7–5.2)	(0.016–0.200)	(0.01–0.43)	
RS-2	6.58	1.41	3.1	0.837	3.55	20
Jan–Feb 1997	(5.77–7.03)	(1.08–1.65)	(0.52–9.8)	(0.301–1.720)	(0.10–9.66)	
RS-3	7.05	1.07	11.4	0.031	0.03	12
Apr–Mar 1997	(6.58–7.50)	(0.98–1.26)	(6.7–19.0)	(0.022–0.064)	(0.01–0.05)	
RS-4	6.43	1.54	1.9	0.551	1.92	34
Nov–Dec 1997	(5.53–7.23)	(0.97–2.07)	(0.3–4.1)	(0.076–2.442)	(0.08–13.02)	
Antarctic Polar Front						
APF-1	6.78	1.24	2.4	0.394	0.08	11
Dec 1997–Jan 1998	(6.02–7.78)	(0.83–1.58)	(0.3–7.9)	(0.115–0.730)	(0.02–0.18)	
APF-2	7.07	1.07	6.7	0.140	0.05	16
Feb–Mar 1998	(6.35–7.66)	(0.76–1.29)	(1.4–1.3)	(0.06–0.335)	(0.02–0.06)	
Arabian Sea						
ARAB-1	7.52	0.85	6.7	0.166	0.53	15
Mar–Apr 1995	(6.82–7.93)	(0.72–1.14)	(2.9–8.7)	(0.085–0.260)	(0.03–1.60)	
ARAB-2	7.59	0.83	6.1	0.177	1.85	7
Jul–Aug 1992	(7.16–7.82)	(0.75–0.92)	(2.8–7.6)	(0.102–0.285)	(0.63–3.48)	
Equatorial Pacific Ocean						
EQP-1	6.93	1.13	10.9	0.074	0.52	17
Mar–Apr 1992	(6.41–7.33)	(1.00–1.24)	(7.3–15.1)	(0.052–0.103)	(0.43–0.65)	
EQP-2	7.10	1.01	7.8	0.117	0.70	20
Sep–Oct 1992	(6.71–7.61)	(0.92–1.12)	(4.3–12.6)	(0.085–0.168)	(0.39–0.89)	

Table 3. Summary of heterotrophic bacteria (HB) parameters used to estimate c_{HB} . n_{HB} : real part of relative refractive index of HB; BA: number of bacteria per unit of volume (cells m^{-3}) $\times 10^{11}$; BV: average biovolume per cell (μm^3) $\times 10^{-2}$. Values are means (min–max) for n_{HB} and means (+1 SE) for BA and BV. Relative biases in percentage for n_{HB} , BA and BV were ± 0.39 , ± 5 and ± 10 , respectively. Cruise details are given in Table 2

Cruise	n_{HB}	BA	BV
RS-1	1.069 (1.061–1.074)	0.92 (0.04)	4.24 (0.12)
RS-2	1.055 (1.047–1.064)	16.1 (2.10)	7.53 (0.26)
RS-3	1.067 (1.060–1.071)	2.92 (0.16)	4.47 (0.15)
RS-4	1.052 (1.039–1.069)	4.17 (0.64)	9.04 (0.47)
APF-1	1.061 (1.048–1.084)	5.20 (0.84)	6.14 (0.67)
APF-2	1.068 (1.059–1.087)	6.31 (0.37)	4.47 (0.23)
ARAB-1	1.081 (1.066–1.092)	12.9 (1.56)	2.89 (0.18)
ARAB-2	1.082 (1.079–1.085)	14.1 (0.91)	2.72 (0.08)
EQP-1	1.064 (1.060–1.070)	6.89 (0.22)	4.97 (0.01)
EQP-2	1.070 (1.066–1.075)	8.55 (0.64)	4.05 (0.01)

Table 4. Linear regression models for estimating covariability between c_{HB} and c_p . Polar comprises RS and APF surveys, and non-polar comprises ARAB and EQP surveys. n: number of data, r^2 : coefficient of determination. M and I are slope and intercept of the model: $c_p = M c_{HB} + I$, respectively. For each regression parameter, statistical significance is indicated at 95% (*) and 99% (**) of probability level

	Polar	Non-polar
n	102	57
r^2	0.36**	0.36**
M	30.20**	10.94**
I	0.148*	0.022

22.5, 37.2, 3 and 3% higher Q_{HB} , σ_{HB} , c_{HB} and c_{HB}/c_p , respectively, compared to a typical microbial population dominated by coccoid morphotypes.

Contribution of HB to horizontal variability of c_p

In general, optical light attenuation due to HB was not the main scattering source affecting c_p spatial variability in surface waters of different tropical, subtropical and Antarctic oceanic domains (Table 4). c_{HB} accounts for approximately 35% of observed variability in c_p for both Antarctic and non-polar regions. The regression slopes confirm that c_{HB} makes a greater contribution to c_p magnitude in non-polar waters than in Antarctic waters. However, the intercept of the $c_p - c_{HB}$ regression curve for the Antarctic group was significantly different from zero ($p < 0.05$). As deduced from the magnitude of standardized multiple regression coefficients (β), BA was the primary factor dictating horizontal variability of c_{HB} in Antarctic ($\beta_{BA} = 0.946$, $\beta_{BV} = 0.146$) and non-polar ($\beta_{BA} = 1.127$, $\beta_{BV} = 0.355$) surveys ($p < 0.01$).

DISCUSSION

The main focus of the present study was to calculate c_{HB} in oceanic regions not investigated before (Southern and Indian oceans) and to evaluate, by comparison with published data, the importance of HB contribution to c_p magnitude and variability in marine waters. This knowledge is necessary to better understand marine ecosystem functions by building more realistic biogeochemical models coupled to optical variables related to HB ecological processes (respiration and synthesis of POC, regulation of the 'biological pump') (Fujii et al. 2007, Claustre et al. 2008). Since c_p is not affected by changes in sunlight geometry (inherent optical property) and is secondarily influenced by the chemical composition of particulates, c_p can be used as a specific proxy of particle concentration per unit of volume in surface marine waters. Given this, changes in bacterial abundance are expected to be reflected in c_p measurements. However, based on transmissometry, can the HB signal be discriminated from other particulate optical targets co-dominating the total beam attenuation coefficient?

Interpretation of our results is organized into 3 sections describing the variation of c_{HB}/c_p due to (1) methodological differences, (2) latitudinal and seasonal variation of c_{HB}/c_p magnitude and (3) $c_{HB} - c_p$ relationships in surface marine waters during Antarctic and non-polar surveys.

Assumptions behind c_{HB} calculations

Analysis of uncertainties associated with c_p estimates is fundamental to evaluate the differences in marine biogeographic zones in terms of HB contribution to c_p and to provide mathematical constraints to the contribution of other c_p components (e.g. detritus) with even larger uncertainties than c_{HB} (Claustre et al. 1999, Grob et al. 2007). Assumptions regarding bacterial cell shape (spherical versus cylindrical) are not expected to modify the observed trends in c_{HB}/c_p between Antarctic and non-polar oceanic domains. Indeed, we calculated that less than 5% change in c_{HB}/c_p was due to variations in bacterial cell shape. Clavano et al. (2007) suggested that the influence of particle shape on attenuation or scattering properties is minor when particles have a mean cell size comparable with the transmissometer wavelength. Our estimations of c_{HB} values included a variable bacterial cell size and refractive index (real part). Among the cited references, this $d - n_{HB}$ parameterization is uncommon since additional optical measurements are usually required (e.g. spectrophotometric absorption cross section) (Green et al. 2003). Most of the published studies

report σ_{HB} values based on constant d and n_{HB} values (Chung et al. 1998, Claustre et al. 1999, Oubelkheir et al. 2005, Grob et al. 2007). Our observed range of d values (0.34 and 0.67 μm) is generally lower than the mean bacterial diameter (0.55 μm) commonly chosen by other authors for calculations based on field measurements (Claustre et al. 1999) or theoretical models (Stramski & Kiefer 1990, Oubelkheir et al. 2005). Therefore, with the only exception being results obtained from the New England continental shelf (Green et al. 2003), we suggest that HB geometrical cross sections have been overestimated in most $c_{\text{HB}}/c_{\text{p}}$ calculations reported in the literature ($\Delta c_{\text{HB}}/c_{\text{p}}$ up to ~ 1.5 -fold). Considering a total estimation error of $\sim 0.4\%$, an uncertainty comparable with that suggested by Aas (1996), our estimated n_{HB} values (1.039 and 1.092) were within the range (1.077 to >1.10) reported for shelf waters influenced by sediments (Green et al. 2003), and for bacterial lab cultures with samples collected in the California Coastal Current (1.042 to 1.068) (Stramski & Kiefer 1990) and Bermuda Sea (1.037 to 1.038) (Jonasz et al. 1997). Note that the methodological procedure to derive n_{HB} differed between Green et al. (2003) (flow cytometry and Mie theory), Stramski & Kiefer (1990) (Mie theory) and Jonasz et al. (1997) (immersion refractometry and ADA, 10% accuracy). Considering the sum of uncertainties due to n_{HB} , BA, and d , our calculations of c_{HB} ($c_{\text{HB}}/c_{\text{p}}$) had a relative error of $\pm 36.1\%$ ($\pm 36.6\%$) and $\pm 31.7\%$ ($\pm 37.7\%$) for samples collected in Antarctic and non-polar waters, respectively.

Contribution of HB to c_{p} magnitude

For the first time and based on 6 Antarctic and 4 non-polar oceanographic surveys, we present evidence that HB contribution to c_{p} is smaller at high latitudes (>2 -fold) than at low and mid latitudes. In fact, analysis of the regression intercept for c_{p} – PCSA curves and probabilistic distribution of c_{p}/PCSA confirmed the greater importance of additional optical components driving c_{p} in Antarctic samples compared with tropical and sub-tropical waters (Appendix 1, Fig. A1).

In general, the number of bacterial cells per unit of volume was a major factor, compared with bacterial cell size spectrum, shape or chemical composition, in explaining observed $c_{\text{HB}}/c_{\text{p}}$ differences. These results agree with the fact that numerical abundance of microorganisms (d , range 0.2 to 100 μm) is more sensitive ($\text{BA} \propto d^{-4}$) to d modifications than the geometric section of the same microorganisms ($S_{\text{HB}} \propto d^2$) (Kiefer 1984). On average, bacterial size and n_{HB} were also different between Antarctic and non-polar surveys, but we suggest that this variation was caused by the

anomalous bacterial dynamics of the Ross Sea. The Ross Sea seems to exhibit a large bacterial bloom (BV changes ~ 4 -fold) not seen elsewhere in Antarctic waters (Ducklow et al. 2001b). Our $c_{\text{HB}}/c_{\text{p}}$ estimations for the sampling locations were generally below 10% and were not necessarily affected by trophic status (chl levels). In the Pacific Ocean (Grob et al. 2007), $c_{\text{HB}}/c_{\text{p}}$ values of surface tropical and subtropical waters (8.4 to 34.6° S) were never above 15% (6.3 to 13% range), and maximum values were observed at lower latitudes. Likewise, Grob et al. (2007) did not find a clear relationship between the spatial gradients of vertically integrated (0 to 50 m) $c_{\text{HB}}/c_{\text{p}}$ and chl values. Based on average values per survey, $c_{\text{HB}}/c_{\text{p}}$ was consistently lower during ARAB-2 and EQP-2 compared with ARAB-1 and EQP-1, respectively (Table 2). This effect was probably caused by a greater proportion of particulate beam attenuation due to phytoplankton with respect to HB during periods of surface nutrient enrichment (El Niño cold phase and summer monsoons) (Ducklow et al. 1995, 2001a).

Contribution of HB to horizontal variability of c_{p}

Based on datasets analyzed, HB was not the main optical component explaining surface horizontal variability of c_{p} ($\sim 35\%$) measured at 660 nm wave length. In the eastern South Pacific Ocean, spatial variability of c_{p} (at 660 nm) is primarily defined by pigmented particles (*Prochlorococcus*, *Synechococcus* and eukaryotes), especially in areas with higher trophic status (Grob et al. 2007). Although HB only represented a minor fraction of c_{p} magnitude, the influence of bacteria on spatial variability of c_{p} was more important. This can be attributed to the covariation between c_{p} , HB and other optical components such as phytoplankton (Li et al. 2004) and detritus (Abell & Bowman 2005).

CONCLUSION

The magnitude and spatial variability of c_{p} were weakly modulated by HB in surface oceanic waters encompassing a broad latitudinal range. In all samples studied, the contribution of HB to c_{p} was never dominant, and c_{p} response to various HB concentrations was partially indirect and probably overestimated due to the existence of other optical particulate components (e.g. phytoplankton), which correlated with c_{p} and HB abundance. This may restrict the use of beam transmissometers for estimating HB biomass-dependent parameters over relatively small spatial scales (0.1 to 100 km). However, we suggest that averaged $c_{\text{HB}}/c_{\text{p}}$ values weighted over large marine

domains (>1000 km) may be a useful ecological index for discriminating biogeographic regions with different particle dynamics.

Acknowledgements. We appreciate the suggestions from E. Boss and 2 anonymous reviewers that helped to improve the ideas developed in the present work. This study was part of the Palmer-LTER (Long-Term Ecological Research) on the western shelf of the Antarctic Peninsula, funded by NSF grant OPP-02-17282.

LITERATURE CITED

- Aas E (1996) Refractive index of phytoplankton derived from its metabolite composition. *J Plankton Res* 18:2223–2249
- Abell GCJ, Bowman JP (2005) Colonization and community dynamics of class Flavobacteria on diatom detritus in experimental mesocosms based on Southern Ocean seawater. *FEMS Microbiol Ecol* 53:379–391
- Agogué H, Casamayor EO, Bourrain M, Obernosterer I, Joux F, Herndl G, Lebaron P (2005) A survey on bacteria inhabiting the sea surface microlayer of coastal ecosystems. *FEMS Microbiol Ecol* 54:269–280
- Baldwin WW, Bankston PW (1988) Measurement of live bacteria by Nomarski interference microscopy and stereologic methods as tested with macroscopic rod-shaped models. *Appl Environ Microbiol* 54:105–109
- Behrenfeld MJ, Boss E (2006) Beam attenuation and chlorophyll concentration as alternative optical indices of phytoplankton biomass. *J Mar Res* 64:431–451
- Bird DF, Karl DM (1999) Uncoupling of bacteria and phytoplankton during the austral spring bloom in Gerlache Strait, Antarctica Peninsula. *Aquat Microb Ecol* 19:13–27
- Bishop JKB (1999) Transmissometer measurement of POC. *Deep-Sea Res I* 46:353–369
- Bjørnsen PK (1986) Automatic determination of bacterioplankton biomass by image analysis. *Appl Environ Microbiol* 51:1199–1204
- Bricaud L, Beldhomme AL, Morel A (1988) Optical properties of diverse phytoplankton species: experimental results and theoretical interpretation. *J Plankton Res* 10:851–873
- Brown DJ, Vickers GT, Collier AP, Reynolds GK (2005) Measurement of the size and orientation of convex bodies. *Chem Eng Sci* 60:289–292
- Chung SP, Gardner WD, Richardson MJ, Walsh ID, Landry M (1996) Beam attenuation and micro-organisms: spatial and temporal variations in small particles along 140°W during the 1992 JGOFS EqPac transects. *Deep-Sea Res II* 43:1205–1226
- Chung SP, Gardner WD, Landry MR, Richardson MJ, Walsh I (1998) Beam attenuation by microorganisms and detrital particles in the equatorial Pacific. *J Geophys Res* 103(C6):12669–12681
- Claustre H, Morel A, Babin M, Caillaud C and others (1999) Variability in particle attenuation and chlorophyll fluorescence in the tropical Pacific: scales, patterns, and biogeochemical implications. *J Geophys Res* 104(C2):3401–3422
- Claustre H, Huot Y, Obernosterer I, Gentili B, Tailliez D, Lewis M (2008) Gross community production and metabolic balance in the south Pacific Gyre, using a non-intrusive bio-optical method. *Biogeosciences* 5:463–474
- Clavano WR, Boss E, Karp-Boss L (2007) Inherent optical properties of non-spherical marine-like particles: from theory to observation. *Oceanogr Mar Biol Annu Rev* 45:1–38
- Cole J, Findlay S, Pace ML (1988) Bacterial production in fresh and saltwater ecosystems: a cross-system overview. *Mar Ecol Prog Ser* 43:1–10
- Duarte CM, Agustí S, Vaqué D, Agawin NSR, Jordi F, Casamayor EO, Gasol JM (2005) Experimental test of bacteria–phytoplankton coupling in the Southern Ocean. *Limnol Oceanogr* 50:1844–1854
- Ducklow HW, Quinby HL, Carlson CA (1995) Bacterioplankton dynamics in the equatorial Pacific during the 1992 El Niño. *Deep-Sea Res II* 42:621–638
- Ducklow HW, Smith DC, Campbell L, Landry MR, Quinby HR, Steward GF, Azam F (2001a) Heterotrophic bacterioplankton in the Arabian Sea: basinwide response to year-round high primary productivity. *Deep-Sea Res II* 48:1303–1323
- Ducklow HW, Carlson CA, Church M, Kirchman D, Smith D, Steward G (2001b) The seasonal development of the bacterioplankton bloom in the Ross Sea, Antarctica, 1994–1997. *Deep-Sea Res II* 48:4199–4221
- DuRand MD, Olson RJ (1996) Contributions of phytoplankton light scattering and cell concentration changes to diel variations in beam attenuation in the equatorial Pacific from flow cytometric measurements of pico-, ultra- and nanoplankton. *Deep-Sea Res II* 43:891–906
- Fujii M, Boss E, Chai F (2007) The value of adding optics to ecosystem models: a case study. *Biogeosciences* 4:817–835
- Green RE, Sosik HM, Olson RJ (2003) Contributions of phytoplankton and other particles to inherent optical properties in New England continental shelf waters. *Limnol Oceanogr* 48:2377–2391
- Grob C, Ulloa O, Claustre H, Huot Y, Alarcon G, Marie D (2007) Contribution of picoplankton to the total particulate organic carbon concentration in the eastern South Pacific. *Biogeosciences* 4:837–852
- Grossart HP, Kiorboe T, Tang K, Plough H (2003) Bacterial colonization of particles: growth and interactions. *Appl Environ Microbiol* 69:3500–3509
- Jonasz M, Fournier G, Stramski D (1997) Photometric immersion refractometry: a method for determining the refractive index of marine microbial particles from beam attenuation. *Appl Opt* 36:4214–4225
- Katz A, Alimova A, Xu M, Rudolph E and others (2003) Bacteria size determination by elastic light scattering. *IEEE J Sel Top Quant Elect* 9:277–287
- Kiefer DA (1984) Microplankton and optical variability in the sea: fundamental relationships. *Proc SPIE* 489:42–48
- Knap A, Michaels A, Close A, Ducklow H, Dickson H (1994) Protocols for the Joint Global Ocean Flux Study (JGOFS) core measurements. JGOFS Rep No. 19, Reprint of the IOC Manuals and Guides No. 29, UNESCO, Paris
- Li KW, Head EJH, Harrison G (2004) Macroecological limits of heterotrophic bacterial abundance in the ocean. *Deep-Sea Res I* 51:1529–1540
- Loisel H, Morel A (1998) Light scattering and chlorophyll concentration in case 1 waters: a reexamination. *Limnol Oceanogr* 32:847–858
- Mitchell BG, Holm-Hansen O (1991) Bio-optical properties of Antarctic Peninsula waters: differentiation from temperate ocean models. *Deep-Sea Res* 38:1009–1028 V
- Morel A, Ahn Y (1990) Optical efficiency factors of free-living marine bacteria: influence of bacterioplankton upon the optical properties and particulate organic carbon in oceanic waters. *J Mar Res* 48:145–175
- Oubelkheir K, Claustre H, Sciandra A, Babin B (2005) Bio-optical and biogeochemical properties of different trophic regimes. *Limnol Oceanogr* 50:1795–1809

- Quan X, Fry ES (1995) Empirical equation for the index of refraction of seawater. *Appl Opt* 34:3477–3480
- Sieburth JM, Brooks RD, Gessner RV, Thomas CD, Tootle JL (1974) Microbial colonization of marine plant surfaces as observed by scanning electron microscopy. In: Colwell RR, Morita RY (eds) *Effect of the ocean environment on microbial activities*. University Park Press, Baltimore, p 418–432
- Simon M, Azam F (1989) Protein content and protein synthesis rates of planktonic marine bacteria. *Mar Ecol Prog Ser* 51:201–213
- Spinrad RW, Gover H, Ward BB, Codispoti LA, Kullenberg G (1989a) Suspended particle and bacterial maxima in Peruvian coastal waters during cold water anomaly. *Deep-Sea Res* 36:715–733
- Spinrad RW, Yentsch CM, Brown J, Dortch Q, Haugen E, Revelante N, Shapiro L (1989b) The response of beam attenuation to heterotrophic growth in a natural population of plankton. *Limnol Oceanogr* 34:1601–1605
- Stramski D, Kiefer DA (1990) Optical properties of marine bacteria. *Proc SPIE* 1302:250–268
- Stramski D, Kiefer DA (1991) Light scattering by microorganisms in the open ocean. *Prog Oceanogr* 28:343–383
- Stramski D, Kiefer DA (1998) Can heterotrophic bacteria be important to marine light absorption? *J Plankton Res* 20: 1489–1500
- Stramski D, Bricaud A, Morel A (2001) Modeling the inherent optical properties of the ocean based on the detailed composition of planktonic community. *Appl Opt* 40:2929–2945
- Ulloa O, Sathyendranath S, Platt T, Quiñones R (1992) Light scattering by marine heterotrophic bacteria. *J Geophys Res* 97:9616–9629
- Van de Hulst HC (1957) *Light scattering by small particles*. John Wiley and Sons, Chichester
- Wiebe WJ, Pomeroy LR (1972) Microorganisms and their association with aggregates and detritus in the sea: a microscopic study. *Mem Ist Ital Idrobiol* 29(Suppl):325–352

Appendix 1. Proportion of particulate beam attenuation explained by marine heterotrophic marine bacteria with a spherical shape

The response of c_p with respect to HB was examined by plotting c_p as a function of particle cross-sectional area per unit of volume (PCSA), and by analyzing the magnitude of the average attenuation efficiency factor for HB ($c_p/PCSA$) (Behrenfeld & Boss 2006) (Fig. A1).

Although c_p and PCSA of HB were positively related in all studied areas (Fig. A1a,c), the dispersion of points around the regression line of south Antarctic ($c_p = 2.043 \text{ PCSA} \pm 0.256 [1 \text{ SE}] + 0.141 \pm 0.051$) and non-polar ($c_p = 0.78 \text{ PCSA} \pm 0.16 + 0.02 \pm 0.02$) samples was remarkable. This variability along the regression line could be attributed to the influence of additional optical components affecting c_p (e.g. detritus, phytoplankton). Detritus concentration is minimal in Antarctic waters (Mitchell & Holm-Hansen 1991); thus, phytoplankton is probably the main factor responsible for the observed poor fit between c_p and PCSA

in south Antarctic waters. In low and mid latitudes, detritus and phytoplankton are probably the main particulates determining residuals between measured and estimated c_p values as a function of PCSA. The coefficient of determination (r^2) of $c_p - \text{PCSA}$ relationships was not statistically different between south Antarctic and non-polar datasets (Fischer's Z transform test, $p = 0.59$).

According to Van de Hulst (1957), $c_p/PCSA$ should be not be greater than 3.2 when c_p variability is completely explained by the particle polydispersion under study. In our case, this premise was only true for c_p measurements of low and mid latitudes (Fig. A1d). Switching to a cylindrical bacterial shape (cylindrical-to-spherical projected area = 1.12) improved $c_p - \text{PCSA}$ functionality in south Antarctic samples and decreased $c_p/PCSA$ values even though this improvement was minor (~10%).

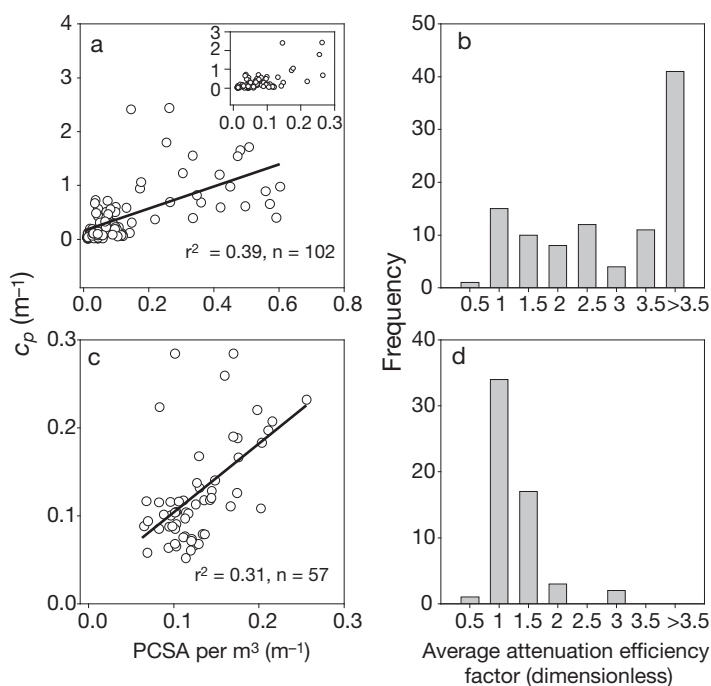


Fig. A1. Relationships between c_p and particle cross sectional area (PCSA) (a,c) and histograms of average attenuation efficiency factor (b,d) for Antarctic (a,b) and non-polar surveys (c,d). Inset in (a) shows PCSA values on an x-axis scale between 0 and 0.3 (y-axis scale, 0 to 3). Note that ranges of c_p and PCSA values of non-polar surveys are smaller compared with Antarctic surveys. Linear regression between c_p and PCSA (solid line) suggest that HB was not a major optical constituent dictating c_p variability in surface marine waters of Antarctic and non-polar surveys

Appendix 2. Variation of cell size distributions of marine heterotrophic bacteria inhabiting oceanic waters and as a function of latitude

For low and mid latitude and Antarctic samples, the probability distribution function (pdf) was computed for each bin of d (pdf_i) by normalizing the number of observations

in each d interval by the total number of observations of the group ($\sum \text{pdf}_i = 1$).

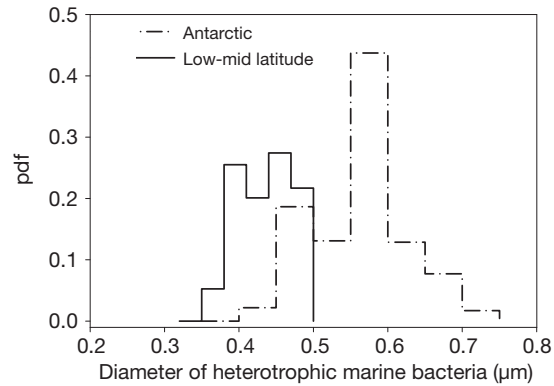


Fig. A2. Probability of finding different bacterial cell size ranges in oceanic domains situated at different latitudes. The diameter of heterotrophic bacteria is derived from biovolume measurements and considers cells with a spherical shape. The mode for Antarctic samples (APF, RS) is 0.55 μm , and for non-polar samples (EQP, ARAB) is 0.44 μm . Peakiness of pdf (kurtosis) is greater in Antarctic samples compared with low and mid latitude samples. APF: Antarctic Polar Front; RS: Ross Sea; EQP: equatorial Pacific; ARAB: Arabian Sea

Editorial responsibility: Rodney Foster,
Suffolk, UK

Submitted: August 19, 2008; Accepted: December 10, 2008
Proofs received from author(s): March 12, 2009